British Journal of Pharmacology

British Journal of Pharmacology (2017) **174** 386–395 386

RESEARCH PAPER

miR-15b mediates oxaliplatin-induced chronic neuropathic pain through BACE1 down-regulation

Correspondence Atsushi Sakai, Department of Pharmacology, Nippon Medical School, 1-1-5 Sendagi, Bunkyo-ku, Tokyo 113-8602, Japan. E-mail: sa19@nms.ac.jp

Received 20 September 2016; **Revised** 11 December 2016; **Accepted** 16 December 2016

Naomi Ito[1,2], Atsushi Sakai[1], Noriko Miyake[3], Motoyo Maruyama[1,4], Hirotoshi Iwasaki[1,2], Koichi Miyake[3], Takashi Okada[3], Atsuhiro Sakamoto[2] and Hidenori Suzuki[1]

[1]Department of Pharmacology, Nippon Medical School, Tokyo, Japan, [2]Department of Anesthesiology, Nippon Medical School, Tokyo, Japan, [3]Department of Biochemistry and Molecular Biology, Nippon Medical School, Tokyo, Japan, and [4]Division of Laboratory Animal Science, Nippon Medical School, Tokyo, Japan

BACKGROUND AND PURPOSE

Although oxaliplatin is an effective anti-cancer platinum compound, it can cause painful chronic neuropathy, and its molecular mechanisms are poorly understood. MicroRNAs (miRNAs) are small non-coding RNAs that negatively regulate gene expression in a sequence-specific manner. Although miRNAs have been increasingly recognized as important modulators in a variety of pain conditions, their involvement in chemotherapy-induced neuropathic pain is unknown.

EXPERIMENTAL APPROACH

Oxaliplatin-induced chronic neuropathic pain was induced in rats by i.p. injections of oxaliplatin (2 mg·kg^{-1}) for five consecutive days. The expression levels of miR-15b and β-site amyloid precursor protein-cleaving enzyme 1 (BACE1 also known as β-secretase 1) were examined in the dorsal root ganglion (DRG). To examine the function of miR-15b, an adeno-associated viral vector encoding miR-15b was injected into the DRG *in vivo*.

KEY RESULTS

Among the miRNAs examined in the DRG in the late phase of oxaliplatin-induced neuropathic pain, miR-15b was most robustly increased. Our *in vitro* assay results determined that BACE1 was a target of miR-15b. BACE1 and miR-15b were co-expressed in putative myelinated and unmyelinated DRG neurons. Overexpression of miR-15b in DRG neurons caused mechanical allodynia in association with reduced expression of BACE1. Consistent with these results, a BACE1 inhibitor dose-dependently induced significant mechanical allodynia.

CONCLUSIONS AND IMPLICATIONS

These findings suggest that miR-15b contributes to oxaliplatin-induced chronic neuropathic pain at least in part through the down-regulation of BACE1.

Abbreviations

AAV, adeno-associated virus; BACE1, β-site amyloid precursor protein-cleaving enzyme 1 (β-secretase 1); DRG, dorsal root ganglion; EGFP, enhanced green fluorescent protein; HRP, horseradish peroxidase; L5, fifth lumbar; LY2886721, N-[3-[(4aS,7aS)-2-amino-4a,5-dihydro-4H-furo[3,4-d][1,3]thiazin-7a(7H)-yl]-4-fluorophenyl]-5-fluoro-2-pyridinecarboxamide; miRNA, microRNA; NRG1, neuregulin 1; TRP, transient receptor potential; UTR, untranslated region

DOI:10.1111/bph.13698

Tables of Links

TARGETS
Enzymes
BACE1

LIGANDS
Oxaliplatin
LY2886721

These Tables list key protein targets and ligands in this article that are hyperlinked to corresponding entries in http://www.guidetopharmacology.org, the common portal for data from the IUPHAR/BPS Guide to PHARMACOLOGY (Southan *et al.,* 2016), and are permanently archived in the Concise Guide to PHARMACOLOGY 2015/16 (Alexander *et al.,* 2015).

Introduction

Peripheral neuropathy is a major dose-limiting adverse effect of several anti-cancer drugs, including platinum compounds (Kim *et al.,* 2015). Patients may experience setbacks in chemotherapy due to peripheral neuropathy, such as being required to decrease their drug dose or frequency, or to switch to other drugs, which can negatively affect the outcome of cancer management (Albers *et al.,* 2014). Oxaliplatin, a third-generation platinum compound, is a key drug used in the treatment of colorectal cancer. However, it can cause two forms of peripheral neuropathy, acute and chronic neuropathy. Acute symptoms appear immediately after oxaliplatin administration and include distal and perioral paresthesia and muscle fasciculation. These symptoms are characteristically triggered by cold stimulation and mediated, at least in part, by transient receptor potential (TRP)A1 and TRPM8 receptors (Kono *et al.,* 2012; Ewertz *et al.,* 2015; Yamamoto *et al.,* 2015). When oxaliplatin causes chronic neuropathy, pain is the most common and severe complaint reported. However, the molecular mechanisms underlying the development of chronic neuropathic pain remain poorly understood.

MicroRNAs (miRNAs) are small non-coding RNAs that regulate gene expression by recognizing the 3′ untranslated regions (UTRs) of mRNAs in a sequence-specific manner and are, therefore, closely involved in diverse pathological conditions, including cancers (Bartel, 2009). Similarly, a variety of miRNAs are causally involved in painful conditions with distinct aetiologies, such as tissue inflammation and traumatic nerve injury (Sakai and Suzuki, 2014). Because the miRNA expression profile extensively varies with the underlying causes, distinct miRNAs appear to be responsible for different pain conditions. Nevertheless, the involvement of miRNA in chemotherapy-induced neuropathic pain has not been reported, although miRNAs have received much attention as therapeutic targets for both pain and cancers.

The miRNA miR-15b is a member of miR-15/107 family, which has a similar sequence in the target-recognizing seed sequence. This miRNA family is implicated in playing a role in cancers and neurodegenerative diseases (Finnerty *et al.,* 2010) and has been shown to target the aspartyl protease β-site amyloid precursor protein-cleaving enzyme 1 (BACE1) (Parsi *et al.,* 2015). In the present study, we found that miR-15b expression was up-regulated in dorsal root ganglion (DRG) neurons following oxaliplatin administration and caused hypersensitivity to mechanical stimuli, possibly through an effect on BACE1.

Methods

Animal model

All experimental procedures were approved by the Animal Experiments Ethical Review Committee of Nippon Medical School (approval number 27–037) and performed in accordance with the guidelines of the International Association for the Study of Pain (Zimmermann, 1983). Animal studies are reported in compliance with the ARRIVE guidelines (Kilkenny *et al.,* 2010; McGrath and Lilley, 2015). A total of 110 male Sprague–Dawley rats (6–7 weeks; 160–230 g; Sankyo Labo Service Corporation, Tokyo, Japan) were randomly subjected to the treatments used in the present study. Rats were housed with access to food and water *ad libitum*. All surgeries were performed under deep anaesthesia induced by an i.p. injection of sodium pentobarbital (50 $mg \cdot kg^{-1}$) or by isoflurane inhalation (2–3%). Rats were killed by exsanguination when under deep anaesthesia. To produce oxaliplatin-induced peripheral neuropathy, a stock solution of oxaliplatin was diluted with 5% glucose solution (2 $mg \cdot mL^{-1}$) and injected i.p. at a dose of 2 $mg \cdot kg^{-1}$ for five consecutive days. This rat model of pain has been in use for several years (Zheng *et al.,* 2011). Control animals were injected with vehicle (1 $mL \cdot kg^{-1}$). The BACE1 inhibitor N-[3-[(4aS,7aS)-2-amino-4a,5-dihydro-4H-furo[3,4-d][1,3]thiazin-7a(7H)-yl]-4-fluorophenyl]-5-fluoro-2-pyridinecarboxamide (LY2886721) was dissolved in 6.7% DMSO and 5% Tween 20 in saline and was injected i.p. at a dose of 10 $mg \cdot kg^{-1}$. Vehicle was injected as a control.

To inject adeno-associated virus (AAV) vectors, the paraspinal muscles were separated from the vertebrae, and a small part of the vertebra overlying the fifth lumbar (L5) DRG was removed to expose the ganglion. The AAV vector (5 μL) was slowly injected into the L5 DRG using a microsyringe with a 27-gauge needle. This focal AAV6 vector injection was previously shown to introduce transgenes specifically into L5 DRG neurons of all sizes (Sakai *et al.,* 2013). The *in vivo* transduction of the AAV vectors into the DRG neurons was confirmed using an enhanced green fluorescent protein (EGFP) immunofluorescence assay.

Behavioural test

Paw withdrawal responses to mechanical stimuli were measured using a set of von Frey filaments (Muromachi Kikai, Tokyo, Japan). Each rat was placed on a metallic mesh floor covered with a plastic box, and a von Frey filament was

applied from underneath the mesh floor to the plantar surface of the hind paw. The weakest force (g) inducing withdrawal of the stimulated paw at least three times in five trials was referred to as the paw withdrawal threshold. These behavioural tests were assessed by an investigator blinded to the treatments of the rats.

Quantitative PCR

For quantitative PCR analysis, all procedures were performed according to the manufactures' protocols. Total RNA was extracted from the L5 DRG using RNAiso Plus (Takara Bio, Shiga, Japan). Total RNA (10 ng) was reverse-transcribed with a mature miR-15b-specific stem-loop primer using a TaqMan MicroRNA Reverse Transcription kit. PCR mixtures were prepared with TaqMan Universal PCR Master Mix and miR-15b-specific TaqMan probe and primers included in the TaqMan MicroRNA Assays. PCR amplifications were performed at 95°C for 10 min, followed by 40 cycles of 95°C for 15 s and 60°C for 1 min. The amplification efficiency for one PCR cycle was obtained by assaying serially diluted samples (four points at dilutions of 1:5), and the relative expression was calculated.

Plasmids

To produce an AAV plasmid vector expressing miR-15b (pAAV-miR-15b), miR-15b and its flanking region were amplified from the rat genome using forward (5′-CCATGGGATTGACTTAGACC-3′) and reverse (5′-CCCTGTCACACTAAAGCAG-3′) primers with EcoRI restriction sites attached at the 5′ ends. The amplified DNA fragment was subcloned into the EcoRI site of the AAV vector plasmid pAAV/ASA (Miyake *et al.,* 2014), which contains a CAG promoter upstream of the transgene and an EGFP gene driven by the B19 promoter. As a control, pAAV-EGFP (Noro *et al.,* 2004), which expresses EGFP driven by a CAG promoter, was used.

A plasmid vector encoding firefly luciferase followed by *BACE1* 3′-UTR was constructed. The *BACE1* 3′-UTR sequence was amplified from rat DRG-derived cDNA. A forward (5′-GGAGGCCAGTGGGCAGATGA-3′) and reverse (5′-CCTCAGCCCTACAATATTCT-3′) primer pair with SpeI restriction sites attached at the 5′ ends was used. The PCR products were subcloned into the SpeI site after the luciferase gene of the pMIR-REPORTER. The miR-15b seed sequence within the 3′-UTR sequence was mutated using a QuikChange II XL Site-Directed Mutagenesis kit and the primers 5′-GTCAGGGCTGAAGCTTAAGGTGCAACATTTCC-AACTCAAG-3′ and 5′-CTTGAGTTGGAAATGTTGCACCTTA-AGCTTCAGCCCTGAC-3′.

AAV vector production

Serotype 6 AAV vectors were produced by adenovirus-free triple transfection with AAV vector, AAV packaging (pRepCap 6as, provided by DW Russell) (Rutledge *et al.,* 1998) and helper plasmids (pHelper) at a ratio of 1:1:1. For miR-15b-expression and control AAV vectors, plasmids were co-transfected into HEK293 cells using calcium phosphate precipitation as previously described (Miyake *et al.,* 2012). Six hours after transfection, the culture medium was replaced with fresh medium, and cells were then cultured for 3 days at 37°C under 5% CO_2 in a humidified atmosphere. Cells were suspended in PBS and freeze-thawed three times. Cell debris was pelleted at 6500 x *g* for 30 min at 4°C, and AAV vectors were purified by ammonium sulphate precipitation and iodixanol continuous gradient centrifugation. The AAV vector titre was determined by quantitative PCR. For use, each AAV vector was diluted with PBS to approximately 5×10^{13} vector genomes·mL^{-1}.

Immunofluorescence

The L5 DRG sections were pre-incubated in PBS containing 5% normal donkey serum and 0.2% Triton X-100 for 30 min and then incubated with rabbit anti-GFP antibody (1:1000) at 4°C overnight. Sections were washed in PBS and then incubated with a secondary antibody labelled with Alexa Fluor 488 at room temperature for 1 h. Images were captured using a high-resolution digital camera equipped with a computer (Olympus, Tokyo, Japan).

Luciferase assay

The activities of firefly and *Renilla* luciferases were measured using the Dual-Glo Luciferase Assay System. The HEK293T cells were seeded onto a 96-well plate (2×10^4 cells per well). The next day, cells were co-transfected with pMIR luciferase reporter, pGL4.74[hRluc/TK] and pAAV-miR-15b using Lipofectamine 2000. Two days after transfection, Dual-Glo luciferase reagent was added to each well, and firefly luminescence was measured using a Wallac 1420 $ARVO_{MX}$ plate reader (PerkinElmer, Waltham MA). Then, Dual-Glo Stop & Glo reagent was added to each well, and *Renilla* luminescence was measured. Firefly luminescence was divided by *Renilla* luminescence and then the luminescence of control pMIR for normalization.

RT-PCR of microdissected samples

Single cells were obtained by laser capture microdissection. The L5 DRG was excised under isoflurane anaesthesia and then rapidly frozen in OCT compound using dry ice/acetone. The DRG was sectioned (20 μm) using a cryostat (Leica, Wetzlar, Germany), and sections were mounted onto RNase-free PEN membrane glass slides (Leica). The sections were incubated in RNAlater solution for 2 min at room temperature. After being washed with RNase-free water for 1 min on ice, the sections were stained with toluidine blue (0.05%, pH 4.1) for 15 s on ice to visualize the DRG neurons. After again being washed with RNase-free water for 1 min on ice, the sections were dried with a hair drier. Single DRG neurons were obtained using a laser microdissection system (LMD7000; Leica) and were processed with a Single Cell-to-CT kit according to the corresponding manufacturer's protocol (Thermo Fisher Scientific). The single DRG neuron was lysed, and the DNA was degraded with DNase I. Reverse transcription reaction of the lysed sample for BACE1 analysis was performed using reagents in the Single Cell-to-CT kit, and the reaction for miR-15b was performed using a TaqMan MicroRNA Reverse Transcription Kit and mature miRNA-specific stem-loop primers, including miR-15b (TaqMan MicroRNA Assays). The reverse transcription product was pre-amplified using cocktails supplied in the TaqMan Gene Expression assays for BACE1, or those supplied in the TaqMan MicroRNA assays for miRNA-specific primer pairs (including miR-15b). PCR amplification of the diluted pre-

amplified product was conducted as described in the *Quantitative PCR* section. Signal intensity was considered positively detected when it was 10-fold greater than that of the negative control.

Immunoblotting

The L5 DRG was sonicated in 10 mM Tris–HCl (pH 7.2) containing 250 mM sucrose, 10 mM HEPES, 10 mM EDTA and protease inhibitor cocktail or was homogenized in the Cell Suspension buffer contained in the *mir*Vana PARIS kit. Tissue lysates were centrifuged at 13 000 × *g* and 4°C for 20 min. Supernatants were electrophoresed on SDS-PAGEs and electroblotted onto PVDF membranes (GE Healthcare Life Sciences, Pittsburgh, PA). Membranes were incubated with an anti-BACE1 (1:200) or an anti-GAPDH (1:1000) antibody at 4°C overnight followed by horseradish peroxidase (HRP)-conjugated secondary antibody (1:2000). Membranes were then processed for chemiluminescence (ECL Prime Western Blotting Detection Reagents), which was detected by a C-DiGit Blot Scanner (LI-COR Biotechnology, Lincoln, NE). GAPDH was used as a loading standard. Optical densities of bands were quantified using ImageJ (National Institutes of Health, Bethesda, MD).

Data and statistical analyses

Data are expressed as the mean ± SEM. Expression values for the results of quantitative PCR, luciferase and immunoblotting assays are expressed as percentages of controls because they were assayed as relative quantities. SPSS software (version 18, IBM, Armonk, NY) and KyPlot (version 5, KyenceLab, Tokyo, Japan) were used for statistical analysis. The data and statistical analysis comply with the recommendations on experimental design and analysis in pharmacology (Curtis *et al.*, 2015). Normality of the data was assessed by the Shapiro–Wilk test. Paired *t*-tests were used for normally distributed data sets, and the Mann–Whitney *U*-test or Steel test for multiple comparisons if normality was rejected. Equality of variance was assessed by Levene's test. Data were analysed by Student's unpaired *t*-test to determine difference between the groups. Values of $P < 0.05$ were considered statistically significant.

Materials

Oxaliplatin (Elplat) was obtained from Yakult, (Tokyo, Japan), and LY2886721 from AdooQ Bioscience (Irvine, CA). TaqMan MicroRNA Reverse Transcription kits, TaqMan Universal PCR Master Mix, TaqMan MicroRNA assays, pMIR-REPORTER, rabbit anti-GFP antibody, secondary antibody labelled with Alexa Fluor 488, Lipofectamine 2000, RNAlater, Single Cell-to-CT kits and mirVana PARIS kits were purchased from Thermo Fisher Scientific (Waltham, MA). The pHelper and QuikChange II XL Site-Directed Mutagenesis kits were obtained from Agilent Technologies (Santa Clara, CA). The Dual-Glo Luciferase Assay System and pGL4.74[hRluc/TK] were purchased from Promega (Fitchburg, WI). The OCT compound was obtained from Sakura Finetek (Tokyo, Japan), and the protease inhibitor cocktail from Roche Diagnostics (Basel, Switzerland). The anti-BACE1 antibody was purchased from Sigma-Aldrich (St. Louis, MO), while the anti-GAPDH antibody and HRP-conjugated secondary antibody were from Cell Signaling Technology (Danvers, MA). The ECL Prime Western Blotting Detection reagents were obtained from GE Healthcare Life Sciences (Pittsburgh, PA).

Results

miR-15b expression is up-regulated in the DRG in oxaliplatin-induced neuropathy

Oxaliplatin administration for five consecutive days caused significant mechanical allodynia that appeared 7 days after the first injection and persisted for at least 28 days (Figure 1A). To examine the involvement of miRNAs in oxaliplatin-induced chronic neuropathy, a main dose-limiting factor in clinical practice, miRNA expression levels were assessed 28 days after the first oxaliplatin administration. We first addressed the expression changes of several miRNAs up-regulated in the DRG after nerve injury that we had observed in our previous study (Sakai *et al.*, 2013). Among the miRNAs examined, miR-15b was most robustly up-regulated in the L5 DRG (Figure 1B). We next determined the time course for the miR-15b expression change. The expression level of miR-15b was not significantly altered in the early phase of oxaliplatin-induced peripheral neuropathy, whereas it was significantly increased in the late phase (Figure 1C).

miR-15b overexpression causes mechanical allodynia

To examine the involvement of miR-15b in mechanical allodynia, we increased the expression of miR-15b in the DRG neurons of intact rats using a serotype 6 AAV vector. Injection of the AAV vector encoding both miR-15b and EGFP into the L5 DRG induced EGFP expression in L5 DRG neurons of all sizes 7 days after the injection (Figure 2A), as previously shown (Towne *et al.*, 2009). The AAV vector injection also increased miR-15b expression (Figure 2B), and miR-15b overexpression caused significant mechanical allodynia in intact rats (Figure 2C).

miR-15b targets the 3′-UTR of BACE1

Because miRNAs block the translation of certain mRNAs by binding to their 3′-UTR sequences, we searched for potential candidate genes targeted by miR-15b using TargetScan (http://www.targetscan.org). Among the predicted targets, we focused on BACE1 because BACE1-null mice show an increased sensitivity to pain (Hu *et al.*, 2006). We first determined whether miR-15b actually targeted the 3′-UTR sequences of *Bace1* mRNA. The *Bace1* 3′-UTR sequence was inserted downstream of the luciferase gene in a plasmid vector. The activity of luciferase with the *Bace1* 3′-UTR sequence was consistently decreased by miR-15b (Figure 3A). To identify the miR-15b binding sequence within the 3′-UTR, we mutated the predicted *Bace1* seed sequences. The activity of luciferase with a mutated 3′-UTR sequence was no longer decreased by miR-15b (Figure 3A). Furthermore, the miR-15b binding sites were well conserved among mammals (Figure 3B).

A single DRG neuron captured using laser microdissection was analysed to examine the expression profiles of miR-15b

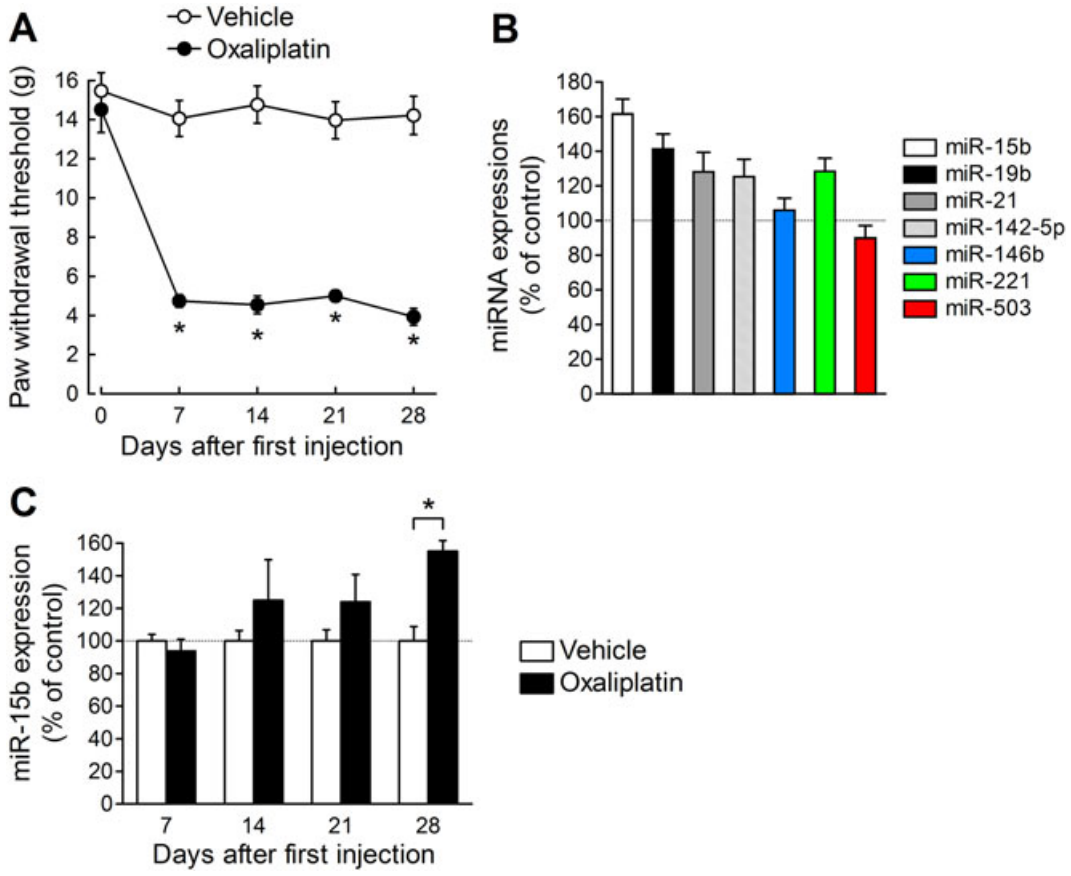

Figure 1

miR-15b expression is increased in the chronic neuropathic pain observed following oxaliplatin administration. (A) Paw withdrawal responses to mechanical stimuli were evaluated before and after vehicle ($n = 10$) or oxaliplatin ($n = 9$) injection for five consecutive days. *$P < 0.05$ versus the value of vehicle by the Mann–Whitney *U*-test. (B) Expression levels of the miRNAs that were up-regulated after traumatic nerve injury in our previous study (Sakai *et al.,* 2013) were examined in the L5 DRG 28 days after the first oxaliplatin injection ($n = 5$). (C) Expression levels of miR-15b in the L5 DRG on the indicated days after the first oxaliplatin injection ($n = 5$ for days 7, 14 and 21; $n = 6$ for day 28). *$P < 0.05$ by Student's unpaired *t*-test.

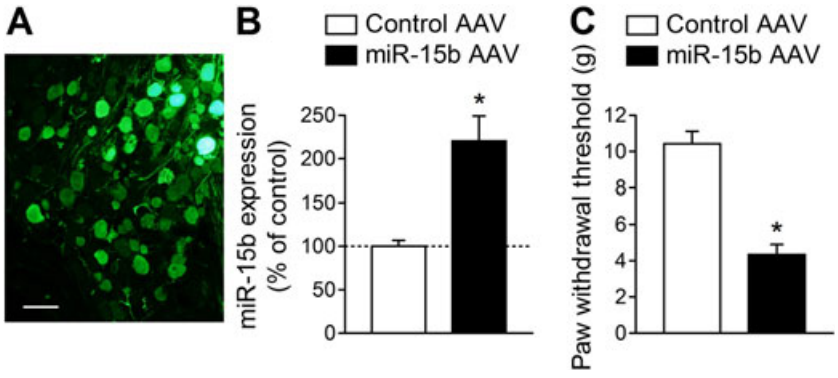

Figure 2

Overexpression of miR-15b in DRG neurons causes mechanical allodynia. (A) Representative image of EGFP immunofluorescence in the intact L5 DRG 7 days after AAV vector injection. Scale bar, 100 μm. (B) Levels of miR-15b expression were examined in the L5 DRG 7 days after control ($n = 6$) or miR-15b ($n = 7$) AAV injection. *$P < 0.05$, by Student's unpaired *t*-test. (C) Paw withdrawal thresholds in response to mechanical stimuli were evaluated 7 days after the AAV injection. *$P < 0.05$ by the Mann–Whitney *U*-test ($n = 5$).

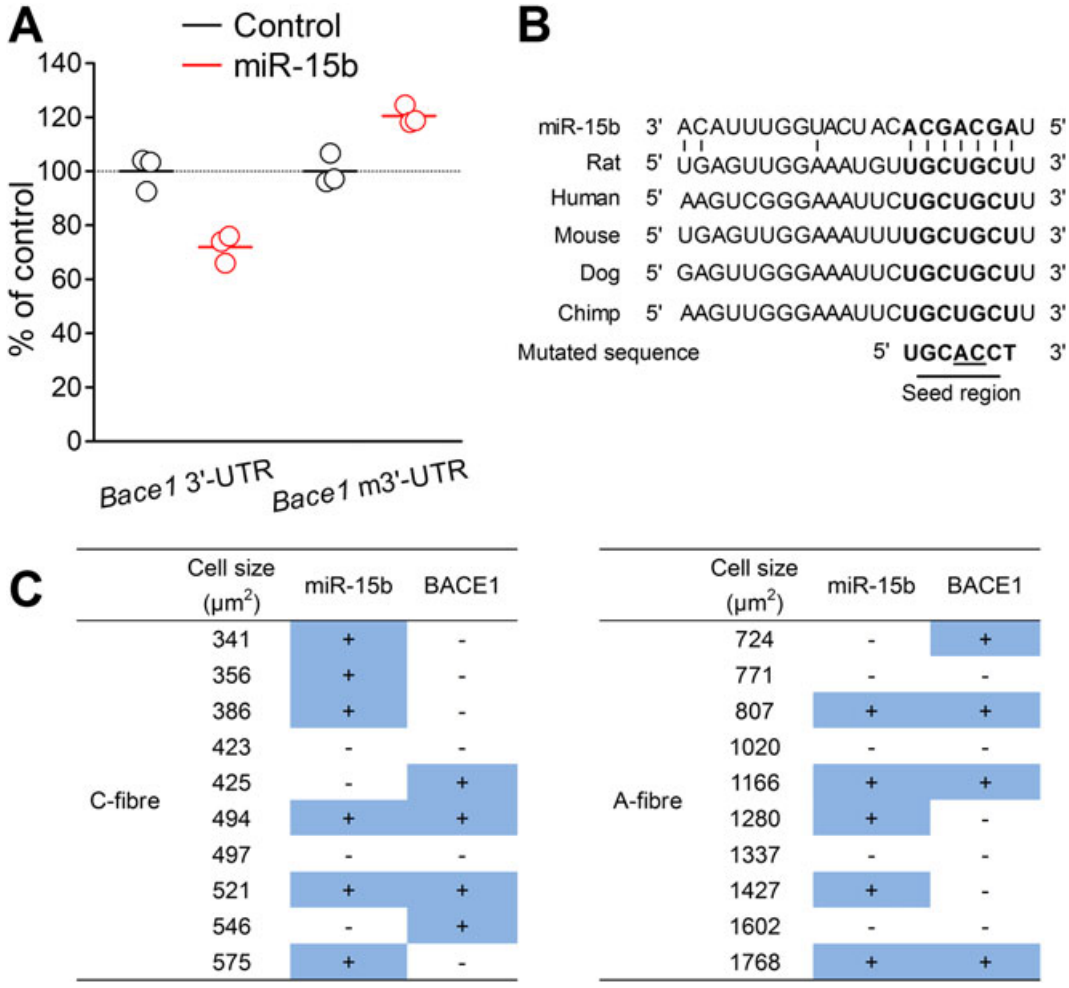

Figure 3

miR-15b targets the conserved *Bace1* 3′-UTR sequence. (A) Activity of luciferase with *Bace1* 3′-UTR or mutated (m) 3′-UTR in 293 T cells co-transfected with control or an miR-15b-expressing plasmid vector (n = 3 culture wells independently transfected within one experiment). (B) Schematic representation of the miR-15b sequence and its target sequence within the *Bace1* 3′-UTRs of mammals. Seed sequences are indicated by bold letters. (C) Expression profiles of miR-15b and BACE1 in single DRG neurons of the indicated cell sizes. Single DRG neurons were captured by laser microdissection, and gene expression was assessed using RT-PCR. DRG neurons with a cell size smaller or larger than 600 μm^2 were considered putative C-fibre and A-fibre neurons respectively.

and BACE1 in L5 DRG neurons. The expression of BACE1 and miR-15b was detected using RT-PCR in both small-sized cells, putative non-myelinated C-fibre neurons, and in medium/large-sized cells, putative myelinated A-fibre DRG neurons (Figure 3C). The miR-15b expression was detected in five out of eight BACE1-positive DRG neurons.

BACE1 is down-regulated in the DRG after oxaliplatin administration and miR-15b overexpression

BACE1 protein expression was examined in the DRG following oxaliplatin administration. On day 28 after the first oxaliplatin injection, but not before day 28, BACE1 expression was significantly decreased in the DRG (Figure 4A). The overexpression of miR-15b in intact rats decreased BACE1 expression 7 days after the AAV injection (Figure 4B).

BACE1 inhibitor causes mechanical allodynia

To examine the effect of BACE1 inhibition on pain behaviour, the BACE1 inhibitor LY2886721 was injected i.p. into intact rats. LY2886721 (10 mg·kg^{-1}) exerted no acute effect on paw withdrawal threshold to mechanical stimuli (Figure 5A). However, 6 h after the injection, LY2886721 caused persistent mechanical allodynia, which was no longer present 3 days after the injection (Figure 5A). This pronociceptive effect of LY2886721 occurred in a dose-dependent manner (Figure 5B).

Discussion

In this study, miR-15b was up-regulated in DRG neurons in the late, but not early, phase of oxaliplatin-induced peripheral neuropathy. Because miR-15b overexpression alone was sufficient to cause significant mechanical allodynia in intact

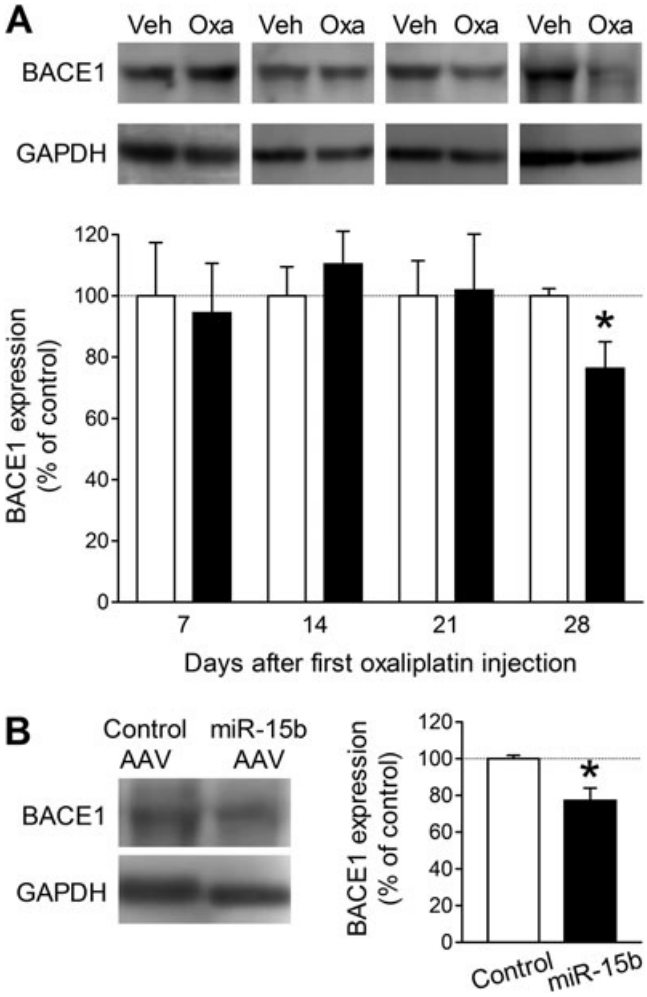

Figure 4

Oxaliplatin and miR-15b reduce BACE1 protein expression. (A, B) Expression levels of BACE1 protein in the L5 DRG after vehicle (Veh) or oxaliplatin (Oxa) injections on the indicated days (A; $n = 5$), and 7 days after control (B; $n = 5$) or miR-15b (B; $n = 6$) AAV injections. GAPDH was used as a loading standard. *$P < 0.05$ by Student's unpaired *t*-test.

rats, miR-15b probably contributed to the chronic mechanical allodynia observed in oxaliplatin-induced neuropathy. In addition to causing mechanical allodynia, oxaliplatin reportedly induces chronic cold allodynia (Xiao *et al.,* 2012). In the present study, although we did not examine whether miR-15b up-regulation and subsequent BACE1 inhibition induced cold allodynia, the involvement of several molecules whose functions are regulated by BACE1 has been previously examined in this noxious cold sensation. For example, intrathecal injection of TNFα, whose receptor is regulated by BACE1, affects the response in the cold-plate test (Nakanishi *et al.,* 2016).

The late onset of the increase in miR-15b expression suggests the specific contribution of miR-15b to the maintenance of oxaliplatin-induced neuropathic pain, although it remains unclear which factors induced increased miR-15b expression in the late phase. However, LPS has been shown to increase miR-15b expression in a trophoblast cell line (Yang *et al.,* 2016). Consistent with this result, LPS-activated intracellular signalling molecules, ERK and NFκB induce miR-15b expression through c-Rel and CREB in HeLa cells (Zhu *et al.,* 2016). The expression of miR-15b is also induced by platelet-derived growth factor in human pulmonary artery smooth muscle cells (Kim and Kang, 2013).

BACE1 down-regulation by miR-15b contributes to the painful peripheral neuropathy induced by oxaliplatin, although other target genes may also be involved. We found that miR-15b was co-expressed in more than half of the DRG neurons expressing BACE1, and the time course for BACE1 down-regulation paralleled that for miR-15b up-regulation after oxaliplatin injection, suggesting that miR-15b can regulate BACE1 expression in a cell-autonomous manner. Our results indicate that miR-15b directly targeted the 3′-UTR sequence of *BACE1* because the mutated *BACE1* 3′-UTR sequence was no longer decreased by miR-15b. The conservation of target 3′-UTR sequences among mammals observed in the present study suggested the functional importance of BACE1 regulation by miR-15b. Consistent with this result, miR-15b overexpression or oxaliplatin administration decreased BACE1 expression in DRG neurons *in vivo*. Furthermore, systemic administration of the BACE1 inhibitor induced mechanical allodynia. BACE1 is a membrane-anchored aspartyl protease that cleaves a variety of substrates involved in neuronal functions, including myelination (Kuhn *et al.,* 2012; Vassar *et al.,* 2014; Barão *et al.,* 2016). Indeed, BACE1 expression was detected in the present study in putative myelinated DRG neurons. It was previously reported that BACE1-null mice show hypomyelination of sciatic nerves (Hu *et al.,* 2006). BACE1 expression was also detected in the present study in the small DRG neurons that are generally thought to represent non-myelinated nociceptive neurons. Thus, BACE1 may contribute not only to the myelination but also to the nociception of peripheral sensory neurons.

Neuregulin 1 (NRG1) is the best characterized substrate of BACE1 in peripheral neurons. BACE1-mediated processing of NRG1 leads to its interaction with neighbouring ErbB family receptors, which are expressed in Schwann cells. Interestingly, oxaliplatin was reported to reduce NRG1 expression in the sciatic nerve (Tsutsumi *et al.,* 2014). Reduced axonal NRG1 causes a decrease in the nerve conduction velocity that is associated with hypomyelination in sciatic nerves (Michailov *et al.,* 2004). Transgenic mice expressing dominant-negative ErbB-4 in myelinating cells, such as Schwann cells, also display hypomyelination in peripheral sensory axons (Chen *et al.,* 2006). However, the roles of NRG1 in nociception are conflicting. Dominant-negative ErbB-4 mice exhibit hypersensitivity to mechanical, but not thermal, stimulation, although a causal relationship of the hypomyelination to mechanical pain has not yet been shown. By contrast, NRG1 ablation results in reduced sensitivity to noxious mechanical stimuli (Fricker *et al.,* 2009).

BACE1 may also contribute to oxaliplatin-induced peripheral neuropathy through other mechanisms. BACE1 is known to cleave the Na_V β2 subunit (Wong *et al.,* 2005; Gersbacher *et al.,* 2010), which regulates cell surface

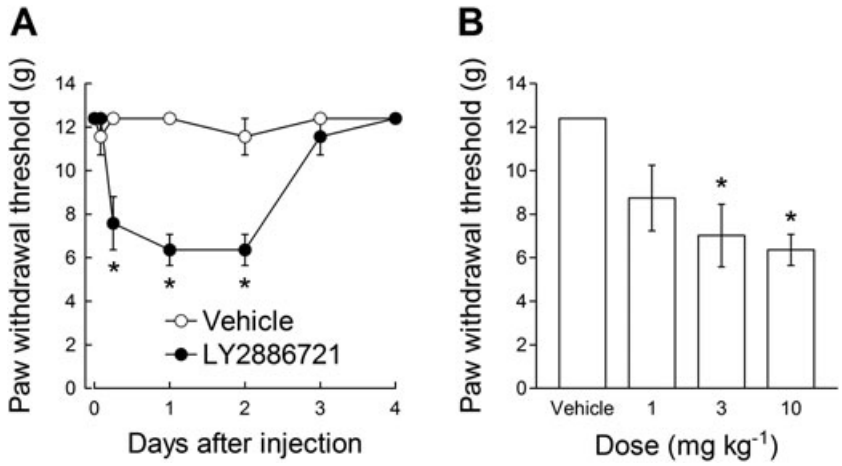

Figure 5

BACE1 inhibition induces mechanical allodynia. (A, B) Paw withdrawal thresholds in response to mechanical stimuli were evaluated in rats after i.p. injection of the BACE1 inhibitor LY2886721 (10 mg·kg^{-1}). (A) Behavioural tests were performed at 2 h, 6 h and 1–4 days after injection. *$P < 0.05$, by the Mann–Whitney *U*-test ($n = 5$). (B) Dose-dependent effect of LY2886721 1 day after injection ($n = 5$). *$P < 0.05$ compared with vehicle, by the Steel test.

expression of voltage-gated sodium channel α subunits (Lopez-Santiago *et al.,* 2006). Thus, BACE1 can modulate the expression of channels and neuronal activity (Lopez-Santiago *et al.,* 2006; Kim *et al.,* 2007). BACE1-null mice show neuronal hyperexcitability associated with increased sodium channel activity (Hu *et al.,* 2010). In addition, Na_V β2-null mice show less severe neuropathic pain after traumatic nerve injury (Pertin *et al.,* 2005). BACE1 was also reported to modulate the expression of TNF receptor 1 (TNFR1), which is a critical mediator of inflammatory processes. TNFR1 expression is increased in BACE1 knockout mice and by a BACE1 inhibitor in wild-type mice independent of the proteolysis of the receptor (Liu *et al.,* 2016).

In conclusion, our results indicated that miR-15b-mediated BACE1 down-regulation may contribute to the pain observed in the chronic phase of oxaliplatin-induced peripheral neuropathy.

Acknowledgements

This work was supported by a Grant-in-Aid for Scientific Research (C) (grant number 25462454 to A.S.) from the Japan Society for the Promotion of Science and by a grant from the Ministry of Education, Culture, Sports, Science and Technology-Supported Programme for the Strategic Research Foundation at Private Universities, 2008–2012, Japan (grant number S0801035 to H.S.).

Author contributions

N.I., A.S., A.S. and H.S. designed and analysed the experiments and wrote the manuscript. N.I., A.S., H.I. and M.M. performed the animal experiments and microdissections. N.I. and A.S. performed the qPCR, immunofluorescence and luciferase assays. N.M., M.M., K.M. and T.O. produced the AAV vectors.

Conflict of interest

The authors declare no conflicts of interest.

Declaration of transparency and scientific rigour

This Declaration acknowledges that this paper adheres to the principles for transparent reporting and scientific rigour of preclinical research recommended by funding agencies, publishers and other organisations engaged with supporting research.

References

Albers JW, Chaudhry V, Cavaletti G, Donehower RC (2014). Interventions for preventing neuropathy caused by cisplatin and related compounds. Cochrane Database Syst Rev 3: CD005228.

Alexander SPH, Fabbro D, Kelly E, Marrion N, Peters JA, Benson HE *et al.* (2015). The concise guide to PHARMACOLOGY 2015/16: enzymes. Br J Pharmacol 172: 6024–6109.

Barão S, Moechars D, Lichtenthaler SF, De Strooper B (2016). BACE1 physiological functions may limit its use as therapeutic target for Alzheimer's disease. Trends Neurosci 39: 158–169.

Bartel DP (2009). MicroRNAs: target recognition and regulatory functions. Cell 136: 215–233.

Chen S, Velardez MO, Warot X, Yu ZX, Miller SJ, Cros D *et al.* (2006). Neuregulin 1-erbB signaling is necessary for normal myelination and sensory function. J Neurosci 26: 3079–3086.

Curtis MJ, Bond RA, Spina D, Ahluwalia A, Alexander SPA, Giembycz MA *et al.* (2015). Experimental design and analysis and their reporting: new guidance for publication in BJP. Br J Pharmacol 172: 3461–3471.

Ewertz M, Qvortrup C, Eckhoff L (2015). Chemotherapy-induced peripheral neuropathy in patients treated with taxanes and platinum derivatives. Acta Oncol 54: 587–591.

Finnerty JR, Wang WX, Hébert SS, Wilfred BR, Mao G, Nelson PT (2010). The miR-15/107 group of microRNA genes: evolutionary biology, cellular functions, and roles in human diseases. J Mol Biol 402: 491–509.

Fricker FR, Zhu N, Tsantoulas C, Abrahamsen B, Nassar MA, Thakur M *et al.* (2009). Sensory axon-derived neuregulin-1 is required for axoglial signaling and normal sensory function but not for long-term axon maintenance. J Neurosci 29: 7667–7678.

Gersbacher MT, Kim DY, Bhattacharyya R, Kovacs DM (2010). Identification of BACE1 cleavage sites in human voltage-gated sodium channel beta 2 subunit. Mol Neurodegener 5: 61.

Hu X, Hicks CW, He W, Wong P, Macklin WB, Trapp BD *et al.* (2006). Bace1 modulates myelination in the central and peripheral nervous system. Nat Neurosci 9: 1520–1525.

Hu X, Zhou X, He W, Yang J, Xiong W, Wong P *et al.* (2010). BACE1 deficiency causes altered neuronal activity and neurodegeneration. J Neurosci 30: 8819–8829.

Kilkenny C, Browne W, Cuthill IC, Emerson M, Altman DG (2010). Animal research: reporting *in vivo* experiments: the ARRIVE guidelines. Br J Pharmacol 160: 1577–1579.

Kim S, Kang H (2013). miR-15b induced by platelet-derived growth factor signaling is required for vascular smooth muscle cell proliferation. BMB Rep 46: 550–554.

Kim DY, Carey BW, Wang H, Ingano LAM, Binshtok AM, Wertz MH *et al.* (2007). BACE1 regulates voltage-gated sodium channels and neuronal activity. Nat Cell Biol 9: 755–764.

Kim JH, Dougherty PM, Abdi S (2015). Basic science and clinical management of painful and non-painful chemotherapy-related neuropathy. Gynecol Oncol 136: 453–459.

Kono T, Satomi M, Suno M, Kimura N, Yamazaki H, Furukawa H *et al.* (2012). Oxaliplatin-induced neurotoxicity involves TRPM8 in the mechanism of acute hypersensitivity to cold sensation. Brain Behav 2: 68–73.

Kuhn PH, Koroniak K, Hogl S, Colombo A, Zeitschel U, Willem M *et al.* (2012). Secretome protein enrichment identifies physiological BACE1 protease substrates in neurons. EMBO J 31: 3157–3168.

Liu L, Fissel JA, Tasnim A, Borzan J, Gocke A, Calabresi PA *et al.* (2016). Increased TNFR1 expression and signaling in injured peripheral nerves of mice with reduced BACE1 activity. Neurobiol Dis 93: 21–27.

Lopez-Santiago LF, Pertin M, Morisod X, Chen C, Hong S, Wiley J *et al.* (2006). Sodium channel β2 subunits regulate tetrodotoxin-sensitive sodium channels in small dorsal root ganglion neurons and modulate the response to pain. J Neurosci 26: 7984–7994.

McGrath JC, Lilley E (2015). Implementing guidelines on reporting research using animals (ARRIVE etc.): new requirements for publication in BJP. Br J Pharmacol 172: 3189–3193.

Michailov GV, Sereda MW, Brinkmann BG, Fischer TM, Haug B, Birchmeier C *et al.* (2004). Axonal neuregulin-1 regulates myelin sheath thickness. Science 304: 700–703.

Miyake K, Miyake N, Yamazaki Y, Shimada T, Hirai Y (2012). Serotype-independent method of recombinant adeno-associated virus (AAV) vector production and purification. J Nippon Med Sch 79: 394–402.

Miyake N, Miyake K, Asakawa N, Yamamoto M, Shimada T (2014). Long-term correction of biochemical and neurological abnormalities in MLD mice model by neonatal systemic injection of an AAV serotype 9 vector. Gene Ther 21: 427–433.

Nakanishi M, Nakae A, Kishida Y, Baba K, Sakashita N, Shibata M *et al.* (2016). Go-sha-jinki-Gan (GJG) ameliorates allodynia in chronic constriction injury model mice via suppression of TNF-α expression in the spinal cord. Mol Pain 12: 1–16.

Noro T, Miyake K, Suzuki-Miyake N, Igarashi T, Uchida E, Misawa T *et al.* (2004). Adeno-associated viral vector-mediated expression of endostatin inhibits tumor growth and metastasis in an orthotropic pancreatic cancer model in hamsters. Cancer Res 64: 7486–7490.

Parsi S, Smith PY, Goupil C, Dorval V, Hébert SS (2015). Preclinical evaluation of miR-15/107 family members as multifactorial drug rargets for Alzheimer's disease. Mol Ther Nucleic Acids 4: e256.

Pertin M, Ji RR, Berta T, Powell AJ, Karchewski L, Tate SN *et al.* (2005). Upregulation of the voltage-gated sodium channel β2 subunit in neuropathic pain models: characterization of expression in injured and non-injured primary sensory neurons. J Neurosci 25: 10970–10980.

Rutledge EA, Halbert CL, Russell DW (1998). Infectious clones and vectors derived from adeno-associated virus (AAV) serotypes other than AAV type 2. J Virol 72: 309–319.

Sakai A, Suzuki H (2014). Emerging roles of microRNAs in chronic pain. Neurochem Int 77: 58–67.

Sakai A, Saitow F, Miyake N, Miyake K, Shimada T, Suzuki H (2013). miR-7a alleviates the maintenance of neuropathic pain through regulation of neuronal excitability. Brain 136: 2738–2750.

Southan C, Sharman JL, Benson HE, Faccenda E, Pawson AJ, Alexander SPH *et al.* (2016). The IUPHAR/BPS Guide to PHARMACOLOGY in 2016: towards curated quantitative interactions between 1300 protein targets and 6000 ligands. Nucleic Acids Res 44: D1054–D1068.

Towne C, Pertin M, Beggah AT, Aebischer P, Decosterd I (2009). Recombinant adeno-associated virus serotype 6 (rAAV2/6)-mediated gene transfer to nociceptive neurons through different routes of delivery. Mol Pain 5: 52.

Tsutsumi K, Yamashita Y, Ushio S, Kawashiri T, Kaname T, Fujita S *et al.* (2014). Oxaliplatin induces hypomyelination and reduced neuregulin 1 expression in the rat sciatic nerve. Neurosci Res 80: 86–90.

Vassar R, Kuhn PH, Haass C, Kennedy ME, Rajendran L, Wong PC *et al.* (2014). Function, therapeutic potential and cell biology of BACE proteases: current status and future prospects. J Neurochem 130: 4–28.

Wong HK, Sakurai T, Oyama F, Kaneko K, Wada K, Miyazaki H *et al.* (2005). β Subunits of voltage-gated sodium channels are novel substrates of β-site amyloid precursor protein-cleaving enzyme (BACE1) and γ-secretase. J Biol Chem 280: 23009–23017.

Xiao WH, Zheng H, Bennett GJ (2012). Characterization of oxaliplatin-induced chronic painful peripheral neuropathy in the rat and comparison with the neuropathy induced by paclitaxel. Neuroscience 203: 194–206.

Yamamoto K, Chiba N, Chiba T, Kambe T, Abe K, Kawakami K *et al.* (2015). Transient receptor potential ankyrin 1 that is induced in dorsal root ganglion neurons contributes to acute cold hypersensitivity after oxaliplatin administration. Mol Pain 11: 69.

Yang M, Chen Y, Chen L, Wang K, Pan T, Liu X *et al.* (2016). miR-15b-AGO2 play a critical role in HTR8/SVneo invasion and in a model of angiogenesis defects related to inflammation. Placenta 41: 62–73.

Zheng H, Xiao WH, Bennett GJ (2011). Functional deficits in peripheral nerve mitochondria in rats with paclitaxel- and oxaliplatin-evoked painful peripheral neuropathy. Exp Neurol 232: 154–161.

Zhu B, Ye J, Ashraf U, Li Y, Chen H, Song Y *et al.* (2016). Transcriptional regulation of miR15b by c-Rel and CREB in Japanese encephalitis virus infection. Sci Rep 6: 22581.

Zimmermann M (1983). Ethical guidelines for investigations of experimental pain in conscious animals. Pain 16: 109–110.